The bulging effect and its relevance in high power laser beam welding

The bulging effect and its relevance in high power laser beam welding

Antoni Artinov[1], Xiangmeng Meng[1], Nasim Bakir[1], Ömer Üstündağ[1], Marcel Bachmann[1], Andrey Gumenyuk[1,2], Michael Rethmeier[3,1,2]

[1]Bundesanstalt für Materialforschung und -prüfung (BAM), Unter den Eichen 87, 12205 Berlin, Germany

[2]Fraunhofer Institute for Production Systems and Design Technology, Pascalstraße 8-9, 10587 Berlin, Germany

[3]Institute for Machine Tools and Factory Management, Technische Universität Berlin, Pascalstraße 8-9, 10587 Berlin, Germany

antoni.artinov@bam.de

Abstract. The present work deals with the recently confirmed widening of the weld pool interface, known as a bulging effect, and its relevance in high power laser beam welding. A combined experimental and numerical approach is utilized to study the influence of the bulge on the hot cracking formation and the transport of alloying elements in the molten pool. A technique using a quartz glass, a direct-diode laser illumination, a high-speed camera, and an infrared camera is applied to visualize the weld pool geometry in the longitudinal section. The study examines the relevance of the bulging effect on both, partial and complete penetration, as well as for different sheet thicknesses ranging from 8 mm to 25 mm. The numerical analysis shows that the formation of a bulge region is highly dependent on the penetration depth and occurs more frequently during partial penetration above 6 mm and complete penetration above 8 mm penetration depth, respectively. The location of the bulge correlates strongly with the cracking location. The obtained experimental and numerical results reveal that the bulging effect increases the hot cracking susceptibility and limits the transfer of alloying elements from the top of the weld pool to the weld root.

1. Introduction

Nowadays, the high power laser beam welding technology is an established tool with increasing capability in joining thick sheets. With available laser powers of up to 100 kW for solid-state lasers, the possible thickness of specimens welded in a single pass has increased up to 50 mm [1, 2]. The comparison of the laser beam welding process with traditional welding processes such as gas metal arc welding (GMAW) and submerged arc welding (SAW) shows the great potential offered by this welding technology. The conventional processes usually require several passes to achieve the desired welding depth, for example, in the manufacturing of thick-walled pipelines for the oil and gas industry. The application of laser beam welding may replace these processes with a single pass and offers the

advantages of high efficiency, high achievable welding speed, high depth-to-width ratio, and narrow heat-affected zone [3].

Despite all advantages of the laser beam welding process, new phenomena occur with increasing welding speed and sheet thickness which are uncommon under conventional welding conditions. Recently, one such phenomena, namely the widening of the weld pool at the solid-liquid interface, known as a bulging effect, was experimentally confirmed [4, 5]. This effect represents a geometric particularity of the weld pool shape and was found to play a crucial role in the formation of defects, such as solidification cracking and porosity. The bulge results as well in a limited transport of alloying elements, e.g. filler wire transfer for wire-based laser beam welding processes, such as hybrid laser-arc welding or laser cold-wire welding. However, the optical inaccessibility of the process and the highly complicated interactions of the involved physical effects make the experimental as well as the numerical investigation of the relevant process variables, leading to the development of the bulging effect, very challenging. This applies as well to the choice of appropriate process parameters such as welding speed, laser power and focal position of the laser beam.

First studies related to the bulging effect and its influence on solidification cracking are found for the electron beam welding process. It was shown that the widened weld pool interface led to a local delay in the solidification behavior, thus increasing the cracking susceptibility in this region [6, 7]. The strong interaction between the widening of the weld pool interface and the crack formation was experimentally confirmed during hybrid laser-GMA welding of thick steel plates as well [8]. The contribution of the bulging effect to the crack formation during laser beam welding has been estimated by various means, e.g. stress distributions [9] or weld pool dynamics [10]. In a detailed study, it was shown that the bulging effect enhances the three most dominant factors, determining the cracking susceptibility of the workpiece, namely the thermal cycle, the temporal mechanical loading, and the local microstructure. Thus, it was concluded that the bulging effect results in a direct increase of the cracking susceptibility during deep penetration laser beam welding [11].

Furthermore, it has been suggested that the bulging effect may be essential for the weld pool dynamics, more specifically the transport of additional alloying elements from the top to the bottom region of the weld pool when filler material is added. As a corollary, it has been argued that the mixing of alloying elements has been limited, leading to inhomogeneous chemical composition of the weld metal and hence non-optimal weld characteristics. Several research works have shown that the widening of the weld pool shape prevents the downward transfer of additional alloying elements to the weld root and so strongly influences the weld seam quality, e.g. the Charpy impact toughness, [12, 13]. It was found that the bulging phenomenon narrows the metal transfer channel between the top and bottom regions of the weld pool, consequently contributing to the higher concentration of filler metal in the top region [14, 15].

To the best of the author's knowledge, there are few studies on the occurrence and relevance of the bulging effect during high power laser beam welding of thick sheets, although similar effects have been observed in several numerical and experimental works, e.g. [16-19]. Based on the literature review, the consequences of the bulging effect in high power laser beam welding of thick sheets are assumed to be twofold. On the one hand the widening of the weld pool interface has the consequence of increased hot cracking susceptibility and on the other hand the limited transport of alloying elements in the molten pool, resulting in an inhomogeneous chemical composition of the weld seam.

The main objective of the present work is the investigation of the two consequences of the bulging effect in deep penetration high power laser beam welding. Thus, a combined experimental and numerical approach was utilized to study the influence of the bulge on both, the hot cracking formation, and the transport of alloying elements in the molten pool. In the analysis, the sheet thickness was varied from 8 mm to 25 mm considering partial and complete penetration. Additionally, an effort has been made to obtain a critical penetration depth above which the bulging effect becomes significant for the weld seam quality.

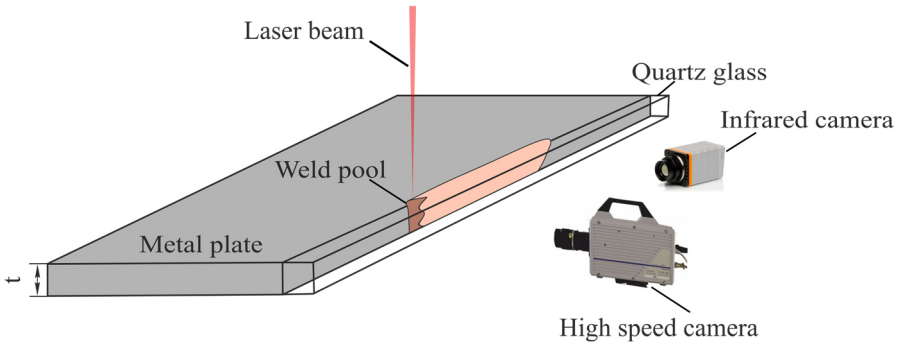

Figure 1: Schema of the experimental setup used for visualization of the weld pool interface in the longitudinal section (t was 15 mm in the complete penetration case and 25 mm in the partial penetration case) according to [5]

2. Experimental study

The experimental investigations presented in this chapter aimed for the prove of the bulge existence and its qualitative observation in the longitudinal section of the weld. The experiments were performed for two different cases, a complete penetration case of 15 mm thick S355 steel sheets and a partial penetration case of 25 mm thick S355 steel sheets. For the partial penetration case a Yb:YAG disk laser TruDisk 16002 from Trumpf has been used with a maximum output power of 16 kW at a wavelength of 1030 nm and a beam parameter product of 8 mm x mrad. In the case of complete penetration, a 20 kW fibre laser IPG YLR-20000 was used with an emission wave-length of 1070 nm and a beam parameter product of 11 mm x mrad. Both laser radiations were transmitted through an optical fiber with a core diameter of 200 µm. A specially designed setup was utilized for the experiments, which was necessary due to the optical inaccessibility of the process. To allow for the observation of the weld pool interface, a butt joint configuration with a transparent quartz glass was considered. The quartz glass used in the present study was selected according to the special requirements for the material properties. It had to provide suitable transparency for the laser wavelength of 1070 nm, meanwhile offering adequate thermal-physical properties, such as low thermal conductivity and thermal expansion coefficient, excellent thermal shock resistance, and high melting temperature. The glass-steel interface was considered as the longitudinal section of the weld. Accordingly, the laser spot was adjusted to lie on the longitudinal plane, so that half of the laser radiation was distributed to the steel plate and the other half to the quartz glass. The weld pool shape was visualized using a high-speed camera and an infrared camera. The sensor in the infrared camera allowed for a detection of a mid-wavelength infrared (MWIR) light, e.g. from 1000 nm up to 5000 nm. The high-speed camera was provided with a filter with a bandwidth of 808±10 nm to reduce the process emissions and thus make it possible to recognize the molten metal. The quartz glass was fully transparent for the complete wavelength range of the infrared camera, thus not interfering with the laser radiation and reflections. A schema of the experimental setup can be seen in Fig. 1.

The experimental setup is based on several previous works with some further improvements and modifications, for more details see [4, 5]. The corresponding process parameters and observations are described in detail in the following sections.

2.1. Complete penetration at 15 mm thick S355 steel sheets

The complete penetration laser beam welding experiment was performed at 15 mm thick S355 steel sheets with welding speed of 2 m/min, laser power of 18 kW, focal position of −5 mm, and focal diameter of 0.56 mm. The real-time observations of the longitudinal section showed that the dimensions of the weld pool interface varied with time along the middle of the penetration depth. The MWIR camera

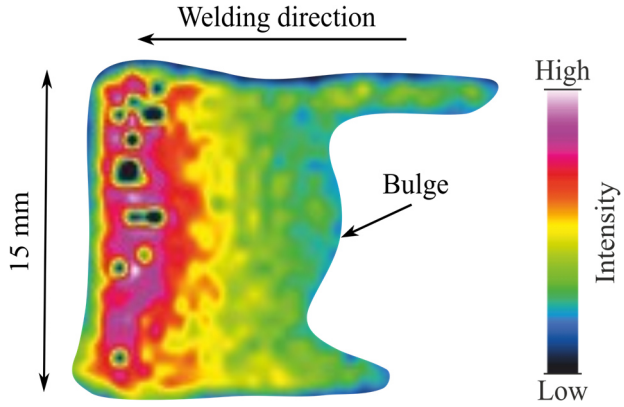

Figure 2: Longitudinal view through the quartz glass using an infrared camera according to [5]

measurement confirmed the bulge location and time variation, as exemplarily shown in Fig. 2 and discussed in more detail in [5]. The observed widening was expected to result in a solidification delay, which could subsequently lead to solidification cracking in this region. This conclusion was in good agreement with post-process results, such as radiographic films and metallographic cross-sections, since in those, the location of the bulge and the crack was nearly the same, see Section 2.2.

2.2. Partial penetration at 25 mm thick S355 steel sheets

The experiment for the partial penetration welding of 25 mm thick sheets was performed using 10 kW laser beam power at a welding speed of 1 m/min. The observations show that the dimensions of the weld pool are depending on the penetration depth. The areas close to the weld pool surface take a teardrop-shape. A bulge region and its temporal evolution were observed approximately in the weld root. Figure 3 a) shows exemplarily a sequence of the longitudinal profile of the weld pool. The observed flow directions are highlighted by red arrows. Two main flow circulations moved the melt from the front to the back of the keyhole ensuring mass conservation. The first circulation occurs in the upper half of the melt pool, which is mainly driven by the recoil pressure and the Marangoni stress on the melt surface. The second circulation is located in the lower half of the melt pool. The liquid metal flowed down from the front wall of the keyhole and then backwards and upwards along the liquid-solid interface, creating a circular flow at the bottom of the melt pool. The two circulations then join in the middle of the melt pool depth and form a narrow region that separates them. The fluid in the narrowed region, which comes together from the upper and lower half of the melt pool, is driven back to the vicinity of the keyhole by the two mentioned vortices. Moreover, the backflows of the melt transport the cooled material into the middle region of the melt pool, thus further reducing the temperature in this region and forming a necking. The strong melt circulation in the keyhole root leads to the elongation of the melt pool in the longitudinal direction and thus to the formation of the bulge region. This bulge promotes solidification cracking by forming a closed region filled with melt that is under tensile stress at the end of the solidification stage [20]. This as well leads to the accumulation of impurities in the final solidification stage and forms low melting phases such as (Fe-S), which additionally contributes to solidification cracking. The tensile stresses in the bulge region could be a result of the restraint condition of the welded parts or of the shrinkage restraint of the relative cold material around the weld root. Fig .3 b) shows an example for solidification crack in the weld root within the bulge region.

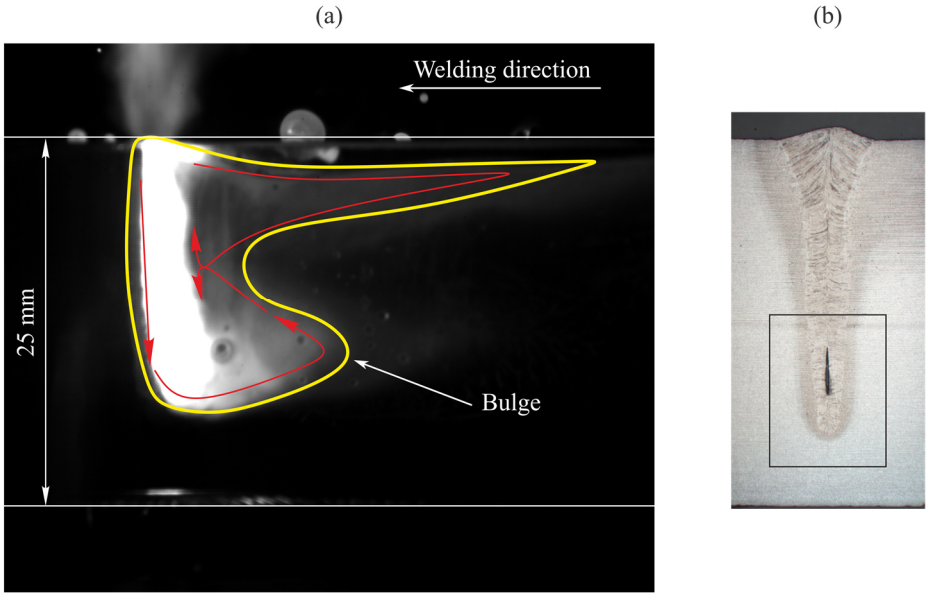

Figure 3: a) Observed melt region and flow pattern in the longitudinal section through the quartz glass using a high-speed camera b) cross-section with solidification crack in the weld root

3. Numerical modelling

This chapter deals with the mathematical description of the weld pool interface. Three numerical models are introduced, allowing for the observation of the bulging effect, more precisely its formation, and its influence on the hot-cracking formation and element transport in the weld pool. The first model was simplified by making use of a fixed keyhole geometry. This permitted for the reproduction of the bulge and the investigation of its effects on solidification cracking. This modelling approach has the advantage of a relatively fast numerical setup and short computational times; however, it is limited to the complete penetration case and does not allow for the investigation of the bulge formation. Thus, a second more sophisticated approach considering a dynamic keyhole was chosen for the investigation of the bulge formation, especially during partial penetration. Such modelling allowed to study not only the bulge formation but as well to estimate a critical penetration depth above which the bulging effect becomes significant for the weld seam quality. The third model was an extension of the dynamic keyhole model developed to simulate the wire feed laser beam welding process. Therefore, it has been applied for the study of the influence of the bulging effect on the transport of alloying elements. It is worth mentioning that the computational intensity of the second and third model exceeds this of the simplified fixed keyhole approach by an order of magnitude, thus increasing the computational time from hours to days.

3.1. Modelling of the bulging effect with a fixed keyhole geometry

The weld pool simulation proposed here aims to obtain a steady-state solution for a weld pool interface containing the bulge region, as observed experimentally in Chapter 2. It should be emphasized here that the model aims at studying the influence of the bulge on the cracking formation and not the formation of the bulge itself. Thus, the model is designed to reproduce the bulge region not quantitatively but rather qualitatively. The weld pool interface was obtained as a solution of the coupled problem, consisting of the mass and energy conservation equations, the Navier-Stokes equations, and the transport equations for the turbulent kinetic energy and turbulent dissipation rate. The model was based on previous research, whereby further improvements, and modifications, allowing for the reproduction of

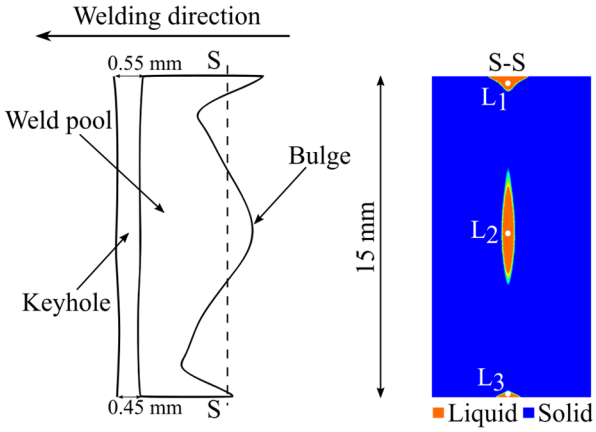

Figure 4: Results from the weld pool computation: (left) three-dimensional longitudinal section of the weld pool in the symmetry plane; (right) liquid metal in the cross-section S-S according to [28]

the bulging effect, has been made. The main assumptions are summarized here, and further details can be obtained from [21-24]. In the numerical model, the workpiece moves relative to the origin of the Cartesian coordinate system, which coincides with the origin of the laser source. A fixed keyhole geometry derived partly from the experimental results was utilized as heat source in the model. This approach was based on the equivalent heat source technique, described in more detail in [25]. The assumption made hereby is that the recoil pressure in the keyhole is perfectly balanced by the surface tension force. The surface temperature of the keyhole was set to the vaporization temperature of the material. According to results obtained with a nearly self-consistent laser beam welding models, e.g. [26, 27], this simplification can be considered as valid assumption. The model accounts for the main physical effects, such as Marangoni and natural convection, latent heat of fusion, and temperature-dependent material properties up to the vaporization temperature. A detailed analysis of the liquid zone showed how crucial the influence of the bulge on the steady-state solidification can be, and more importantly, how critical it can be for the formation of cracks. In Figure 4 the calculated longitudinal section of the weld pool geometry is shown. The weld pool interface was defined by the liquidus isotherm, highlighted by the black curve. For the analysis of the solidification behavior in the bulge region, a cross-section S-S was defined, see left hand side in Fig. 4.

According to the literature review, one of the most important factors for the crack formation is the so-called phenomenon of delayed solidification. This phenomenon, however, is found to be strongly dependent on the weld pool interface and hence on the bulging effect. As the weld pool moves along the welding direction through the cross-section S-S, the regions of liquid and solid metal were obtained from their corresponding overlap. As it can be seen on the right hand side in Fig. 4 there are three locations, highlighted by the points L_1, L_2 and L_3, containing liquid metal on the top, in the centre, and on the bottom of the cross-section. All three locations solidify at the end stage, whereby the delay on the top and bottom regions is due to the thermo-capillary driven flow. However, the solidification delay in the centre is caused by the bulging effect and solidifies at last, making it the most critical location. The presence of liquid material between the grain boundaries in the bulge region at the end stage of the steady-state solidification has a direct impact on the cracking behavior of the part, since the development of solidification cracks requires the presence of a liquid film between the grain boundaries. Thus, it can be concluded, that the bulging effect leads to lower cracking resistance in this particular area.

3.2. Modelling of the bulging effect considering a dynamic keyhole

To simulate a dynamic keyhole behavior, several physical effects have been considered in the second model. The most important of those are summarized in the following. To allow for a self-consistent energy input, a ray tracing algorithm proposed in [28] was implemented. It was used to

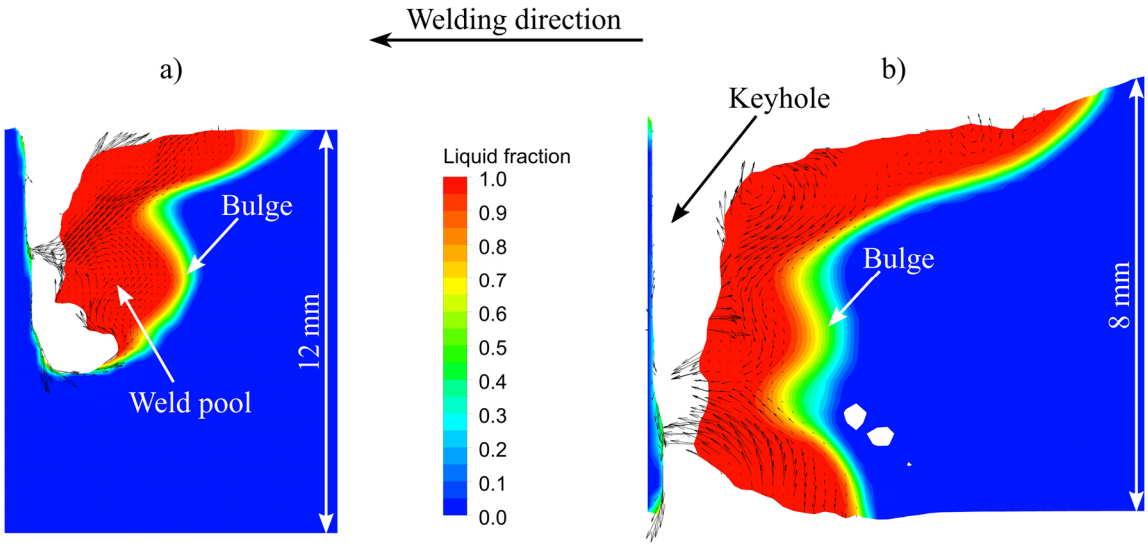

Figure 5: Exemplary results from the weld pool computation: weld pool shape with a bulge during a) partial penetration at 12 mm thick sheet (7.5 kW, 2 m/min, 0 mm focal position); b) complete penetration at 8 mm thick sheet (8 kW, 2 m/min, 0 mm focal position)

calculate the multiple reflection and the Fresnel absorption on the keyhole surface, thus directly contributing to the energy balance on it. The evaporation-induced recoil pressure, which is a dominant driving force for the formation of the keyhole was calculated according to [29]. Additionally, the vapor induced stagnation pressure and shear stresses on the keyhole wall were considered according to [30]. Further details and more complete description of the numerical model can be found in [12].

The dynamic keyhole modelling allowed to study the fluid flow and thus the formation of the bulge. For the estimation of the critical penetration depth above which the bulging effect becomes significant for the weld seam quality, various calculations with different sheet thicknesses for both partial and complete penetration has been performed. It was found that the bulge region forms more frequently during partial penetration above 6 mm penetration depth, see Fig. 5 a). In the complete penetration case, the bulge region formed already at a sheet thickness of 8 mm, see Fig. 5 b). The location of the bulge was, similar to the experimental observations, varying slightly around the middle of the plate thickness. Based on the numerical results it can be suggested that the bulging effect has a non-steady nature and forms randomly along the weld seam. The time-variation of the bulge dimensions is caused by the complex interaction of the main forces, namely the dynamic fluctuations of the keyhole due to the recoil pressure and the surface tension forces. The numerical investigation has shown that the bulging effect becomes more crucial during complete penetration laser beam welding of sheets with a thickness above 8 mm.

3.3. Modelling of the bulging effect considering a dynamic keyhole and filler wire

Commonly, accompanying with the bulging effect, the weld pool will be significantly narrowed at the middle region, which is potentially detrimental for the metal mixing. Based on the model in Section 3.2, a filler wire model was added, and the element transport equations were coupled, aiming at investigating the influence of the bulging effect on the element transport in the wire feed laser beam welding [12, 13]. The base metal used was AISI 304 stainless steel with 8.7% Ni content. The nickel-based Inconel 625 alloy with 58 % Ni content was chosen as filler wire in the current study.

A sufficient mass transfer in vertical direction is required so that the filler material can reach the weld pool bottom. Fig. 6 a) shows the flow of liquid metal in the longitudinal section during partial penetration welding. A strong circulation exists in the upper weld pool. The liquid metal is driven by the recoil

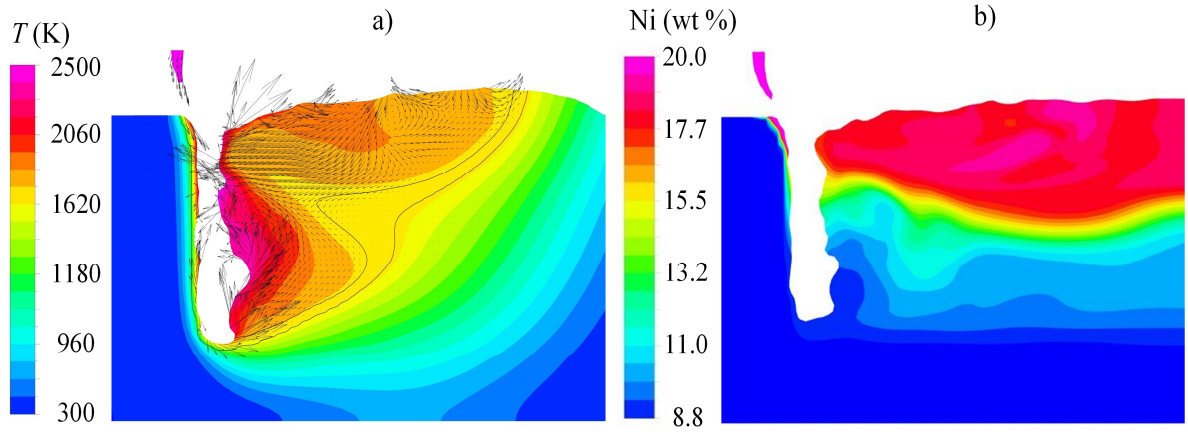

Figure 6: Simulation results of wire feed laser beam welding with bulging formation in partial penetration: a) temperature distribution and velocity field, b) Ni distribution

pressure and the Marangoni stress to flow backward along the free surface, which contributes to the elongated profile of the weld pool and the sufficient metal mixing in the upper region. It should be noted that another dominant circulation occurs in the lower weld pool. The liquid metal near the bottom of the keyhole flows backward and upward along the solid-liquid interface of the weld pool, and subsequently flows toward the keyhole rear wall. It is considered that this lower circulation may directly lead to the occurrence of the bulging effect. As the bulge fully develops, the middle region of the weld pool is significantly narrowed. The weld pool is nearly separated by the narrowed region, so that no downward flow component can be observed. Consequently, the additional Ni from the filler wire concentrates on the upper region of the weld, resulting in an inhomogeneous chemical composition along the thickness of the weld seam, see Fig.6 b).

4. Conclusions

The present work was devoted to the study of the recently confirmed widening of the weld pool interface, known as a bulging effect, and its relevance in high power laser beam welding. A combined experimental and numerical approach was utilized to investigate the influence of the bulge on the solidification cracking formation and the transport of alloying elements in the molten pool.

The following conclusions have been drawn based on the obtained results:

1) A bulge region was found to form during both partial and complete penetration laser beam welding of steel sheets.
2) The bulging effect tends to occur during deep penetration welding, thus playing a more important role in welding workpieces with higher sheet thickness. In the current study, it has been numerically estimated that the bulging will form more frequently during partial penetration above 6 mm and complete penetration above 8 mm penetration depth, respectively.
3) The bulge effect leads to an increase of the cracking susceptibility of the part due to the cause of solidification delay in the cracking region.
4) The bulge effect results in a narrowing of the weld pool interface in the middle region, which may deteriorate the homogeneity of the chemical composition in the weld seam, thus leading to non-optimal weld seam characteristics.

Acknowledgements

This work is funded by the Deutsche Forschungsgemeinschaft (DFG, German Research Foundation) with project numbers 411393804 (BA 5555/5-1) and 416014189 (BA 5555/6-1) and the research project IFG 19582N/ P1241 "Investigation of influence the restraint conditions on hot cracking in laser and laser-hybrid welding of thick structure steels" from the Research Association for steel Application (FOSTA), Düsseldorf. This was supported by the Federal Ministry of Economic Affairs and Energy through the German Federation of Industrial Research Associations (AiF) as part of the programme for promoting industrial cooperative research (IGF) on the basis of a decision by the German Bundestag. The project was carried out at Bundesanstalt für Materialforschung und –prüfung (BAM).

ORCID iDs

Antoni Artinov https://orcid.org/0000-0001-7533-5014
Xiangmeng Meng https://orcid.org/0000-0001-8996-759X
Nasim Bakir https://orcid.org/0000-0001-6847-0365
Ömer Üstündağ https://orcid.org/0000-0002-7352-429X
Marcel Bachmann https://orcid.org/0000-0003-2395-6462
Andrey Gumenyuk https://orcid.org/0000-0002-8420-5964
Michael Rethmeier https://orcid.org/0000-0001-8123-6696

References

[1] Bachmann, M., Gumenyuk, A., & Rethmeier, M. (2016). Welding with high-power lasers: trends and developments. Physics Procedia, 83, 15-25.
[2] Zhang, X., Ashida, E., Tarasawa, S., Anma, Y., Okada, M., Katayama, S., & Mitzutani, M. (2011). Welding of thick stainless steel plates up to 50 mm with high brightness lasers. Journal of Laser Applications, 23(2), 022002.
[3] Ready, J. F., & Farson, D. F. (Eds.). (2001). LIA handbook of laser materials processing.
[4] Artinov, A., Bakir, N., Bachmann, M., Gumenyuk, A., & Rethmeier, M. (2018). Weld pool shape observation in high power laser beam welding. Procedia CIRP, 74, 683-686.
[5] Artinov, A., Bakir, N., Bachmann, M., Gumenyuk, A., Na, S.J., & Rethmeier, M. (2019). On the search for the origin of the bulge effect in high power laser beam welding. Journal of Laser Applications, 31(2), 022413.
[6] Shida, T., Okumura, H., & Kawada, Y. (1979). Effects of welding parameters and prevention of defects in deep penetration electron beam welding of heavy section steel plates, Welding in the world, 17(7/8).
[7] Tsukamoto, S., & Irie, H. (1991). Mechanism of locally delayed solidification in electron beam welding, Welding international, 5(3), 177-183.
[8] Barbetta, L. D., Weingaertner, W. L., Seffer, O., Lahdo, R., & Kaierle, S. (2015). Influence of molten pool geometry and process parameters on solidification cracsk formation in hybrid laser-GMA welding of thick 5L X70 steel plates.

[9] Gebhardt, M., Gumenyuk, A., & Rethmeier, M. (2013). Numerical Analysis of Hot Cracking in Laser-Hybrid Welded Tubes, Advances in Material Science and Engineering.
[10] Wang, H., Nakanishi, M., & Kawahito, Y. (2018). Dynamic balance of heat and mass in high power density laser welding. Opt. Express 26, 6392-6399.
[11] Artinov, A., Bachmann, M., Meng, X., Karkhin, V., & Rethmeier, M. (2020). On the relationshipbetween the bulge effect and the hot cracking formation during deep penetration laser beam welding. Procedia CIRP, 94, 5-10.
[12] Meng, X., Artinov, A., Bachmann, M., & Rethmeier, M. (2020). Numerical study of additional element transport in wire feed laser beam welding. Procedia CIRP, 94, pp.722-725.
[13] Meng, X., Artinov, A., Bachmann, M., & Rethmeier, M. (2020). Theoretical study of influence of electromagnetic stirring on transport phenomena in wire feed laser beam welding. Journal of Laser Applications, 32(2), p.022026.
[14] Meng, X., Bachmann, M., Artinov, A., & Rethmeier, M. (2021). The influence of magnetic field orientation on metal mixing in electromagnetic stirring enhanced wire feed laser beam welding. Journal of Materials Processing Technology, 117135.
[15] Üstündağ, Ö., Gook, S., Gumenyuk, A., & Rethmeier, M. (2019). Mechanical properties of single-pass hybrid laser arc welded 25 mm thick-walled structures made of fine-grained structural steel. Procedia Manufacturing, 36, 112-120.
[16] Cho, W. I., Na, S. J., Thomy, C., & Vollertsen, F. (2012). Numerical simulation of molten pool dynamics in high power disk laser welding, Journal of Materials Processing Technology, 212(1), 262-275.
[17] Sohail, M., Han, S. W., Na, S. J., Gumenyuk, A., & Rethmeier, M. (2015). Numerical investigation of energy input characteristics for high-power fiber laser welding at different positions, The International Journal of Advanced Manufacturing Technology, 80(5-8), 931-946.
[18] Lu, F., Li, X., Li, Z., Tang, X., & Cui, H. (2015). Formation and influence mechanism of keyhole-induced porosity in deep-penetration laser welding based on 3D transient modelling, International Journal of Heat and Mass Transfer, 90, 1143-1152.
[19] Gao, Z., Jiang, P., Mi, G., Cao, L., & Liu, W. (2018). Investigation on the weld bead profile transformation with the keyhole and molten pool dynamic behavior simulation in high power laser welding, International Journal of Heat and Mass Transfer, 116, 1304-1313.
[20] Bakir, N., Artinov, A., Gumenyuk, A., Bachmann, & Rethmeier, M. (2018). Numerical simulation on the origin of solidification cracking in laser welded thick-walled structures. Metals. 8(6): 406.
[21] Beck, M. (1996). Modellierung des Lasertiefschweißens. Teubner.
[22] Rai, R., Kelly, S.M., Martukanitz, R.P., & DebRoy, T. (2008). A convective heat-transfer model for partial and full penetration keyhole mode laser welding of a structural steel. Metallurgical and Materials Transactions A. 39(1), 98–112.
[23] Bachmann, M., Avilov, V., Gumenyuk, A., & Rethmeier, M. (2011). Numerical simulation of full-penetration laser beam welding of thick aluminium plates with inductive support. J. Phys. D Appl. Phys. 035201.
[24] Artinov, A., Bachmann, M., & Rethmeier, M. (2018). Equivalent heat source approach in a 3D transient heat transfer simulation of full-penetration high power laser beam welding of thick metal plates, Int. J. Heat Mass Transf. 122, 1003–1013.
[25] Artinov, A., Karkhin, V., Khomich, P., Bachmann, M., & Rethmeier, M. (2019). Assessment of thermal cycles by combining thermo-fluid dynamics and heat conduction in keyhole mode welding processes. International Journal of Thermal Sciences. 145, 105981.
[26] Tan, W., Bailey, N.S., &Shin, Y.C. (2013). Investigation of keyhole plume and molten pool based on a three-dimensional dynamic model with sharp interface formulation. Journal of Physics D: Applied Physics, 46(5), 055501.
[27] Tan, W., & Shin, Y.C. (2014). Analysis of multi-phase interaction and its effects on keyhole dynamics with a multi-physics numerical model. Journal of Physics D: Applied Physics, 47(34),

345501.
[28] Cho, W. I., Na, S. J., Thomy, C., & Vollertsen, F. (2012). Numerical simulation of molten pool dynamics in high power disk laser welding. Journal of Materials Processing Technology 212, 262-275.
[29] Semak, V., & Matsunawa, A. (1997). The role of recoil pressure in energy balance during laser materials processing. Journal of Physics D-Applied Physics 30, 2541.
[30] Muhammad, S., Han, S. W., Na, S. J., Gumenyuk, A., & Rethmeier, M. (2018). Study on the role of recondensation flux in high power laser welding by computational fluid dynamics simulations. Journal of Laser Application 30, 012013.s